ELSEVIER

Journal of Organometallic Chemistry 491 (1995) 61–69

Journal of Organometallic Chemistry

Reactivity of a (Fe–NO)–(Fe–NO_3) system in the presence of a ferrocene–ferricinium group tethered nearby via a ferrocenyl phosphine linkage (FcP_2): crystal structures of [{$Fe(NO)_2Cl$}$_2$(μ-FcP_2)] and [$Fe(NO)_2(FcP_2)$]

Viateur Munyejabo [a], Jean-Pierre Damiano [a], Michèle Postel [a,*], Corinne Bensimon [b], Jean Louis Roustan [b]

[a] *Laboratoire de Chimie Moléculaire, Unité associée au CNRS 426, Université de Nice-Sophia Antipolis, Parc Valrose, 06108 Nice Cédex 2, France*
[b] *Chemistry Department, University of Ottawa, Ottawa, Ontario KIN 6N5, Canada*

Received 18 July 1994

Abstract

The nitrosyl dimer [{$Fe(NO)_2(Cl)$}$_2$] (**1**) reacts with 1,1′-bis(diphenylphosphino)ferrocene (FcP_2) to yield [$Fe(NO)_2(Cl)$]$_2$(μ-FcP_2) (**2**), the structure of which has been determined. The FcP_2 moiety bridges two $Fe(NO)_2(Cl)$ groups symmetrically. Oxygenation of **1** in the presence of FcP_2 yields [$Fe(NO_3)_2Cl(O_2P_2Fc)$] (**5**): complex **5** catalyses the autoxidation of cyclohexene. It transfers the oxygen atoms of its nitrato groups to phosphines. When allowed to react with an excess of FcP_2, **2** gives [$Fe(NO)_2(FcP_2)$] (**4**); the subsequent formation of [$Fe(NO)Cl_2(FcP_2O)$] (**3**) is attributed to the reaction of **4** with chlorine liberated in situ. The structure of **4** was also determined.

Keywords: Iron; Nitrosyl; Ferrocene ligand; Nitrato complex; X-ray diffraction; Oxidation

1. Introduction

Our efforts to evaluate the susceptibility of nitrosyl ligands to oxidation by dioxygen to nitrite or nitrate [1–5] led us to test an appealing hypothesis, namely that the redox properties of an iron nitrosyl–nitro–nitrate system could be influenced by a ferrocene–ferrocenyl ($Fc–Fc^+$) group tethered nearby via a ferrocenyl phosphine linkage. In this paper, we focus on the chemistry of bis(nitrosyl)iron dimer [{$Fe(NO)_2Cl$}$_2$] (**1**) in the presence of 1,1′-bis(diphenylphosphino)ferrocene (FcP_2).

We have previously reported that the nitrosyl ligands in the bis(nitrosyl)iron dimers [{$Fe(NO)_2X$}$_2$](X = Cl or I) are oxidized by molecular oxygen in the presence of monodentate L (PPh_3 [1], hexamethylphosphoric triamide (HMPA) [2]), or bidentate LL ligands (bipyridine [3,4], dppe [5]) to nitrato and not nitro complexes such as observed with [$Fe(NO_3)X_2L_2$] or [$Fe(NO_3)_2XL_2$] and that these can serve as catalysts for the oxidation of phosphines or olefins. The iron-nitrato–iron-nitrosyl couple thus constitutes an alternative for the activation and transfer of molecular oxygen. Electronic assistance of the $Fc–Fc^+$ couple along the catalytic cycle was hoped for, through increased electron donation to enhance both the O_2 activation step in the catalysis as a result of an activated Fe–NO moiety and the oxygen transfer reaction.

2. Experimental details

Solvents were purified by published procedures and stored under argon. 1,1′-bis(diphenylphosphino)ferrocene was purchased from Aldrich and used without further purification. The dimer [{$Fe(NO)_2Cl$}$_2$] (**1**) [6] and the dioxygenated ligand 1,1′-bis(oxodiphenylphosphoranyl)ferrocene [7] were prepared according to the literature. The preparation of the nitrosyl com-

* Corresponding author.

0022-328X/95/$09.50 © 1995 Elsevier Science S.A. All rights reserved
SSDI 0022-328X(94)05235-2

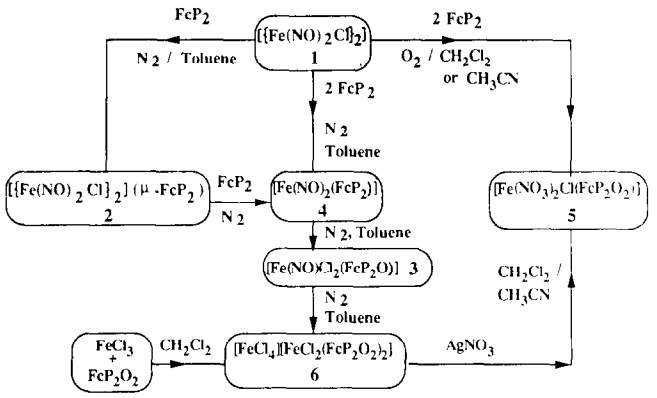

Scheme 1.

plexes was performed under argon using Schlenk tube techniques (Scheme 1).

Elemental analyses were performed by the Service Central de Microanalyses of the CNRS. IR spectra were recorded on a Bruker Fourier transform IFS 45 spectrometer. Electron spin resonance (ESR, spectra were measured on a Bruker 200 SRC spectrometer equipped with a variable-temperature accessory, both in the solid state and in solution. ^{31}P NMR spectra were recorded on a Bruker WH 90 spectrometer. ^{31}P chemical shifts are given in parts per million downfield from external H_3PO_4. Gas chromatography (GC)–mass spectroscopy (MS) analyses were performed on a Finnigan MAT INCOS 500E spectrometer interfaced with a Varian-3400 chromatograph equipped with a DB-5 25 mx0.32 mm capillary column.

2.1. Preparation of $[\{Fe(NO)_2Cl\}_2(\mu\text{-}FcP_2)]$ (2)

The chlorobisnitrosyliron dimer $[\{Fe(NO)_2(Cl)\}_2]$ (0.59 g, 1.95 mmol) was dissolved in toluene (30 ml) and a toluene (40 ml) solution of FcP_2 (0.96 g, 1.73 mmol) was added dropwise. A change from reddish-yellow to violet was observed after complete addition. After 1 h, no precipitate was observed and the reaction mixture was evaporated to dryness to yield a violet powder. This powder was redissolved in 30 ml of toluene, and addition of an equal volume of pentane produced violet parallelepiped-shaped crystals after 1 day at 0°C (1.35 g (91%)). Anal. Found: Fe, 18.73; P, 7.53; Cl, 8.59. $C_{34}H_{28}Cl_2Fe_3N_4O_4P_2$ calc.: Fe, 19.55; P, 7.23; Cl, 8.27%. IR (KBr pellets): ν(NO), 1788 and 1728; ν(P–C) 1099; ν(Fe–Cl), 338 cm^{-1}. ESR (toluene, room temperature (RT):) $g = 2.037$, $a\langle^{31}P\rangle = 21$ G. ^{31}P NMR (toluene, RT): δ 59(s) ppm.

2.2. Preparation of $[Fe(NO)Cl_2(FcPPO)]$ (3) and $[Fe(NO)_2(FcP_2)]$ (4) from 2

0.62 g (0.72 mmol) of **2** was dissolved in toluene (50 ml) and FcP_2 (0.38 g, 0.68 mmol) was added. A change in the solution from violet to red was observed and a green precipitate formed progressively. The reaction mixture was stirred for 1 h and then filtered. To the filtrate was added an equal volume of pentane. After 12 h at 0°C, red crystals of **4** were obtained (0.66 g, 0.98 mmol (67%). Anal. Found: Fe, 15.60; P, 9.35; N, 3.60. $C_{34}H_{28}Fe_2N_2O_2P_2$ calc.: Fe, 16.67; P, 9.24; N, 4.18%. IR (KBr pellets): ν(NO), 1707, 1659; ν(P–C) 1094 cm^{-1}, ^{31}P NMR (CH_2Cl_2, RT): δ 58 (s) ppm. ^1H NMR(CD_2Cl_2, RT): δ 4.3 (m, 8 H, C_5H_4), 7.4 (m, 20 H, C_6H_5) ppm.

The green precipitate was washed with toluene and pentane to afford **3** as a green powder (yield, 0.27 g (27%)). IR (KBr pellets): ν(NO), 1788; ν(P–C) 1094, 1119; ν(PO), 1144; ν(Fe–Cl), 351, 380 cm^{-1}. ESR (CH_2Cl_2, RT): $g = 2.02$. ^{31}P NMR (CH_2Cl_2, RT): δ 34 (P), 40 (PO) ppm.

2.3. Preparation of $[Fe(NO)Cl_2(FcPPO)]$ (3) from $[Fe(NO)_2(FcP_2)]$ (4) and chlorine

Chlorine was bubbled through a methylene chloride solution (60 ml) of the red nitrosyl complex **4** (0.45 g, 0.67 mmol) at RT. After the chlorine addition was completed, the reaction mixture, kept at 4°C for 12 h, turned green. Evaporation of the solvent yielded a greenish residue which was shown by IR and ^{31}P NMR to contain both **3** (40%) and **4** (60%).

2.4. Preparation of $[Fe(NO_3)_2(Cl)(O_2P_2Fc)]$ (5) from 1

Dioxygen was bubbled through an acetonitrile solution (50 ml), containing the chlorobisnitrosyliron dimer **1** (0.800 g, 2.64 mmol) and FcP_2 (2.93 g, 5.29 mmol), at RT for 6 h, resulting in a change from black to brown. After evaporation to dryness and washing with CH_3CN, the brown powder was recrystallized from CH_2Cl_2–Et_2O to yield 3.99 g (98%) of **5** as a crystalline beige powder. Anal. Found: P, 7.82; Cl, 4.42; C, 51.46; N, 3.17. $C_{34}H_{28}ClFe_2N_2O_8P_2$ calc.: P, 7.73; Cl, 4.42; C, 50.94; N, 3.49%. IR (KBr pellets): $\nu(NO_3)$, 1522, 1288, 828; ν(PO), 1148; ν(P–C), 1124; ν(Fe-Cl), 313 cm^{-1}.

2.5. Preparation of 5 from anhydrous $FeCl_3$ via $[FeCl_4][FeCl_2(FcP_2O_2)_2]$ (6)

To a solution of anhydrous $FeCl_3$ (0.49 g, 3.05 mmol) in 30 ml of CH_2Cl_2, a CH_2Cl_2 (30 ml) solution of 1,1'-bis(oxodiphenylphosphoranyl)ferrocene (FcP_2O_2) (1.89 g, 3.04 mmol) was added. The reaction mixture was stirred for 2 h. Recrystallization from CH_2Cl_2–Et_2O yielded 2.25 g of **6** (93%). Anal. Found: Fe, 14.11; P, 8.47; Cl, 14.33; C, 54.77; H, 3.89. $C_{34}H_{28}Cl_3Fe_2O_2P_2$ calc.: Fe, 14.92; P, 8.28; Cl, 14.21; C, 54.55; H, 3.77%. IR (KBr pellets): ν(PO), 1169; ν(P–C), 1134; ν(Fe–Cl), 380 ($FeCl_4^-$), 345 ($FeCl_2(FcP_2O_2)_2^+$) cm^{-1}.

A solution of silver nitrate (0.363 g, 2.14 mmol) in acetonitrile (10 ml) was added dropwise to a solution of **6** (0.8 g, 1.1 mmol) in CH_2Cl_2 (50 ml) at RT. Instantaneous formation of a white precipitate of AgCl resulted; the suspension was stirred for 2 h before filtration. The filtrate was evaporated to dryness. The residue was washed with pentane and dried under vacuum to yield 0.332 g of **5** (89%).

2.6. Molecular structures of $[Fe(NO)_2Cl]_2(\mu\text{-}FcP_2)$ (2) and $[Fe(NO)_2(FcP_2)]$ (4)

2.6.1. Crystal preparation

Air-sensitive crystallographic quality crystals of $C_{34}H_{28}Cl_2Fe_3N_4O_4P_2$ (**2**) ($M = 857$) were isolated as transparent dark-purple parallelepipeds. They were grown by allowing a layer of pentane to diffuse slowly into a solution of **2** in toluene at 0°C, washed with pentane and then dried under a stream of argon. Single red longitudinal crystals of $C_{34}H_{28}Fe_2N_2O_2P_2$ (**4**) ($M = 670$) were obtained similarly by slow diffusion of pentane into a solution of **4** in toluene at 0°C, washed with pentane and then dried under a stream of argon.

2.6.2. Crystallographic data

A summary of crystal data and intensity collections for **2** and **4** is given in Table 1. All the measurements were made on a Rigaku diffractometer with Mo Kα radiation. The unit-cell constants were refined by the least-squares method from angular data for 25 reflections. Based on systematic absences, the space group for **2** was determined to be $P2_1/c$. The systematic absences found for **4** were compatible with space group $C2/c$ or Cc. The structure was solved in both space groups; refinement in Cc indicated that an inversion centre was present and hence the centrosymmetric space group $C2/c$ was preferred for **4**.

The data were collected at −120°C using the ω–2θ scan technique to a maximum 2θ value of 49.9. A total of 3341 (**2**) and 5309 (**4**) reflections were collected; the unique sets contained 3139 (**2**) and 5214 (**4**) reflections.

Table 1
Crystal and data collection parameters for **2** and **4**

	2	**4**
Empirical formula	$C_{34}H_{28}Cl_2Fe_3N_4O_4P_2$	$C_{34}H_{28}Fe_2N_2O_2P_2$
Formula weight	857.01	670.24
Crystal shape	Cube	Cube
Crystal dimensions (mm)	0.2 × 0.2 × 0.2	0.2 × 0.2 × 0.2
Crystal system	Monoclinic	Monoclinic
Space group	$P2_1/c$	$C2/c$
Z	2	8
Number of reflections used for unit-cell dimensions	25	25
2θ range (°)	40–50	40–50
Lattice parameters		
a (Å)	9.4526(19)	33.900 (5)
b (Å)	10.9932(16)	9.077 (1)
c (Å)	17.3475 (20)	19.952 (2)
β (°)	95.739 (12)	105.227 (10)
D calc (g cm^{-3})	1.587	1.503
μ (mm^{-1})	2.97	1.13
$F(000)$	871.01	2759.21
Number of reflections measured	3341	5309
Number of reflections unique	3139	5214
Number of reflections observed	2455	3845
Merging R	0.053	.063
Number of variables	224	380
Number of atoms	39	70
R_f (sign reflection)	0.051	0.051
R_w (sign reflection)	0.033	0.045
R_f (all reflections)	0.075	0.082
R_w (all reflections)	0.033	0.045
Goodness of fit	4.98	3.97
Last difference Fourier map		
Maximum peak (electrons Å^{-3})	0.660	1.010
Minimum peak (electrons Å^{-3})	−0.550	−1.200

Table 2
Atomic parameters and B_{iso} for **2**, where the estimated standard deviations refer to the last digit printed

Atoms (Å^2)	x	y	z	B_{iso}
Fe(1)	0.75095 (9)	0.13227 (8)	0.03069 (5)	2.15 (4)
Fe(2)	1/2	1/2	0	2.53 (6)
P(1)	0.65890 (17)	0.27191 (14)	0.11502 (9)	2.06 (7)
Cl(1)	0.72480 (19)	−0.04912 (14)	0.08274 (9)	3.37 (8)
O(1)	1.0099 (5)	0.2614 (4)	0.03148 (23)	5.4 (3)
O(2)	0.6139 (4)	0.1874 (4)	−0.11805 (21)	4.5 (3)
N(1)	0.9132 (5)	0.1950 (5)	0.03764 (24)	3.3 (3)
N(2)	0.6549 (5)	0.1528 (4)	−0.05552 (24)	2.9 (3)
C(1)	0.4859 (6)	0.2386 (5)	0.1492 (3)	2.3 (3)
C(2)	0.4007 (6)	0.1492 (5)	0.1103 (3)	2.7 (3)
C(3)	0.2665 (6)	0.1258 (6)	0.1339 (3)	3.0 (3)
C(4)	0.2208 (6)	0.1915 (6)	0.1957 (3)	3.5 (3)
C(5)	0.3100 (6)	0.2782 (6)	0.2339 (3)	3.2 (3)
C(6)	0.4407 (6)	0.3023 (6)	0.2130 (3)	2.7 (3)
C(7)	0.7808 (6)	0.2764 (5)	0.2051 (3)	2.1 (3)
C(8)	0.7933 (6)	0.1700 (5)	0.2486 (3)	2.4 (3)
C(9)	0.8911 (6)	0.1655 (6)	0.3143 (3)	3.2 (3)
C(10)	0.9728 (6)	0.2665 (6)	0.3358 (3)	3.4 (3)
C(11)	0.9576 (6)	0.3721 (6)	0.2918 (3)	3.5 (3)
C(12)	0.8630 (6)	0.3762 (5)	0.2257 (3)	2.7 (3)
C(13)	0.6519 (6)	0.4251 (5)	0.757 (3)	2.5 (3)
C(14)	0.5996 (6)	0.5357 (5)	0.1072 (3)	3.0 (3)
C(15)	0.6284 (6)	0.6285 (5)	0.0560 (4)	4.1 (4)
C(16)	0.6956 (6)	0.5819 (5)	−0.0040 (4)	3.9 (3)
C(17)	0.7111 (6)	0.4552 (5)	0.0056 (3)	3.0 (3)

B_{iso} is the mean of the principal axes of the thermal ellipsoid.

The standards were measured after every 150 reflections and no crystal decay was noticed. The data were corrected for Lorentz and polarization effects [8]. Absorption corrections were made. The minimum and maximum transmission factors were 0.091 674 and 0.115 72 for **2**, and 0.6740 and 0.7759 for **4**.

Both structures were solved by direct methods. All the atoms were refined anisotropically except the hydrogen atoms. The hydrogen atoms were found by a difference Fourier map. The final cycle of full-matrix least-squares refinement was based on 2455 (**2**) and 3845 (**4**) observed reflections ($I > 2.5\ \sigma\ (I)$) and 224 (**2**) and 380 (**4**) variable parameters. Weights based on counting statistics were used. The minimum and maximum peaks on the final difference Fourier maps corresponded to 0.66 and −0.55 electrons Å^{-3} for **2** and 1.01 and −1.20 electrons Å^{-3} for **4**.

The atomic positional parameters of **2** and **4** with estimated standard deviations are given in Tables 2 and 3 respectively. The principal bond distances and angles are given in Table 4 (**2**) and 5 (**4**). All the calculations were performed using the NRCVAX crystallographic software package [9].

2.7. General procedure for the oxidation tests

The iron complexes (about 0.1 mmol) were dissolved in 5 ml of CH_2Cl_2 or CH_3CN, and cyclohexene (10

Table 3
Atomic parameters and B_{iso} for **4**, where the estimated standard deviations last digit printed.

Atom (Å^2)	x	y	z	B_{iso}
Fe(1)	0.35943 (3)	0.37040 (10)	0.06112 (5)	1.02 (3)
Fe(2)	0.35414 (3)	0.78859 (10)	0.14882 (4)	1.00 (3)
P(1)	0.38858 (4)	0.73279 (17)	0.06911 (8)	0.98 (5)
P(2)	0.35062 (5)	0.56689 (17)	0.19802 (8)	0.96 (6)
O(1)	0.40014 (16)	0.9852 (6)	0.2517 (3)	2.47 (21)
O(2)	0.27325 (14)	0.8515 (6)	0.0684 (3)	2.43 (21)
N(1)	0.38144 (16)	0.9007 (6)	0.2085 (3)	1.52 (21)
N(2)	0.30698 (16)	0.8209 (6)	0.1018 (3)	1.53 (21)
C(1)	0.44186 (17)	0.7961 (7)	0.0842 (3)	1.32 (23)
C(2)	0.46707 (19)	0.7358 (8)	0.0456 (4)	1.9 (3)
C(3)	0.50661 (22)	0.7890 (10)	0.0549 (4)	2.6 (3)
C(4)	0.52142 (22)	0.8987 (10)	0.1039 (4)	3.1 (4)
C(5)	0.49720 (23)	0.9563 (10)	0.1425 (4)	2.9 (3)
C(6)	0.45698 (21)	0.9053 (8)	0.1331 (4)	2.1 (3)
C(7)	0.36371 (18)	0.8166 (7)	−0.0157 (3)	1.12 (22)
C(8)	0.38451 (18)	0.9133 (7)	−0.0489 (3)	1.27 (24)
C(9)	0.36490 (20)	0.9690 (7)	−0.1137 (3)	1.66 (25)
C(10)	0.32454 (20)	0.9299 (8)	−0.1461 (3)	1.8 (3)
C(11)	0.30349 (19)	0.8377 (8)	−0.1119 (3)	1.80 (25)
C(12)	0.32262 (19)	0.7808 (8)	−0.0472 (3)	1.68 (25)
C(13)	0.39382 (18)	0.5418 (7)	0.0440 (3)	1.25 (24)
C(14)	0.37577 (18)	0.4704 (7)	−0.0207 (3)	1.28 (23)
C(15)	0.38877 (20)	0.3215 (8)	−0.0140 (4)	1.9 (3)
C(16)	0.41546 (20)	0.2979 (8)	0.0528 (4)	1.9 (3)
C(17)	0.41892 (18)	0.4365 (7)	0.0895 (3)	1.34 (25)
C(18)	0.30406 (17)	0.4389 (7)	0.0719 (3)	1.07 (23)
C(19)	0.29957 (19)	0.3014 (8)	0.0351 (3)	1.8 (3)
C(20)	0.32488 (22)	0.1958 (7)	0.0777 (4)	1.9 (3)
C(21)	0.34560 (18)	0.2655 (7)	0.1420 (3)	1.38 (24)
C(22)	0.33282 (18)	0.4166 (7)	0.1383 (3)	1.17 (22)
C(23)	0.31447 (18)	0.5709 (7)	0.2527 (3)	1.23 (22)
C(24)	0.28509 (19)	0.4617 (7)	0.2502 (3)	1.54 (24)
C(25)	0.25867 (18)	0.4719 (8)	0.2927 (3)	1.7 (3)
C(26)	0.26214 (20)	0.5896 (8)	0.3389 (3)	1.8 (3)
C(27)	0.29188 (21)	0.6968 (8)	0.3426 (4)	1.9 (3)
C(28)	0.31791 (19)	0.6872 (7)	0.2989 (3)	1.54 (24)
C(29)	0.39713 (18)	0.4987 (7)	0.2592 (3)	1.45 (23)
C(30)	0.39635 (20)	0.3754 (8)	0.3010 (3)	1.7 (3)
C(31)	0.43217 (22)	0.3266 (9)	0.3469 (4)	2.4 (3)
C(32)	0.46870 (20)	0.4015 (9)	0.3530 (4)	2.3 (3)
C(33)	0.46934 (19)	0.5258 (8)	0.3130 (3)	1.9 (3)
C(34)	0.43356 (19)	0.5754 (8)	0.2657 (3)	1.6 (3)

B_{iso} is the mean of the principal axes of the thermal ellipsoid.

Table 4
Selected bond distances (Å) and bond angles (°) for $[\{Fe(NO)_2Cl\}_2(\mu\text{-}FcP_2)]$ (**2**) with estimated standard deviations in parentheses

Bond distances			
Fe(1)–N(1)	1.674 (5)	N (2)–O (2)	1.178 (6)
Fe(2)–N(2)	1.685 (4)	P (1)–C (1)	1.831 (5)
Fe(1)–Cl(1)	2.2130 (18)	P (1)–C (7)	1.848 (5)
Fe(1)–P(1)	2.3469 (18)	P (1)–C (13) (Cp)	1.815 (5)
N(1)–O(1)	1.183 (7)		
Bond angles			
Fe(1)–N(1)–O (1)	163.3 (5)	P(1)–Fe(1)–N(2)	105.37 (17)
Fe(1)–N(2)–O (2)	163.6 (4)	Cl(1)–Fe(1)–N(2)	114.25 (17)
N(1)–Fe(1)–N (2)	114.62 (22)	Cl(1)–Fe(1)–N(1)	118.71 (18)
O(1)–Fe(1)–O(2)	102.3 (5)	Cl(1)–Fe(1)–P(1)	105.76 (7)
P(1)–Fe(1)–N (1)	94.57 (17)	P(1)–Fe(1)–C(13)	112.00 (19)

mmol) was added to the solution together with octane as an internal standard for GC analyses. The resulting solution was stirred under dioxygen at RT and the oxidation products monitored by GC analysis of aliquots. The oxygenated products were identified by GC–MS analysis and by comparison with authentic samples.

3. Results

3.1. Nitrosyl FcP_2 complexes

3.1.1. Synthesis of $[\{Fe(NO)_2Cl\}_2(\mu\text{-}FcP_2)]$ (2)

When 1,1'-bis (diphenylphosphino)ferrocene (FcP_2) is allowed to react with one equivalent of the $[\{Fe(NO)_2Cl\}_2]$ dimer **1** in toluene at RT, a violet complex **2** is isolated. The analytical data are in consistent with a dinuclear complex. Its IR spectrum showed NO stretches at 1788 and 1728 cm^{-1} and an Fe–Cl stretch at 338 cm^{-1}. Complex **2** is paramagnetic in the solid state and in solution. Its RT ESR spectrum measured in a toluene solution consists of a doublet at $g = 2.037$, with a 21 G hyperfine coupling attributable to the coupling of the unpaired electron with one phosphorus nucleus [10]. The ^{31}P NMR of **2** in CH_2Cl_2 showed a single resonance at 59 ppm (−17 ppm in the free FcP_2 ligand). An X-ray structural investigation unambiguously established **2** as $[\{Fe(NO)_2Cl\}_2(\mu\text{-}FcP_2)]$ in which the FcP_2 ligand acts as a bridge between two iron atoms.

3.1.2. Molecular structure of $[\{Fe(NO)_2Cl\}_2(\mu\text{-}FcP_2)]$ (2)

The molecular structure of **2** is shown in Fig. 1 with selected bond lengths and bond angles listed in Table 4. The FcP_2 bridges two $Fe(NO)_2Cl$ moieties using its two diphenylphosphino groups. The ferrocene iron atom, Fe(2), lies on a crystallographic inversion centre.

Table 5
Selected bond distances (Å) and bond angles (°) for [Fe $(NO)_2$ (P_2Fc)] (**4**) with estimated standard deviations in parentheses

Bond distances			
Fe(2)–N(1)	1.653 (6)	P(1)–C(1)	1.843 (6)
Fe(2)–N(2)	1.654(5)	P(1)–C(7)	1.845 (6)
Fe(2)–P(1)	2.2635(18)	P(1)–C(13)(Cp)	1.826 (6)
Fe(2)–P(2)	2.2560(18)	P(2)–C(22)(Cp)	1.808 (6)
N(1)–O(1)	1.203(7)	P(2)–C(23)	1.842 (6)
N(2)–O(2)	1.195(7)	P(2)–C(29)	1.830 (6)
Bond angles			
Fe(2)–N(1)–O(1)	177.8(5)	P(2)–Fe(2)–N(2)	104.56 (20)
Fe(2)–N(2)–O(2)	176.8(5)	P(1)–Fe(2)–P(2)	101.66 (6)
O(1)–Fe(2)–O(2)	122.9(1)	P(1)–Fe(2)–N(1)	110.47 (19)
N(1)–Fe(2)–N(2)	125.1(3)	P(1)–Fe(2)–N(2)	104.94 (10)
P(2)–Fe(2)–N(1)	108.61 (19)		

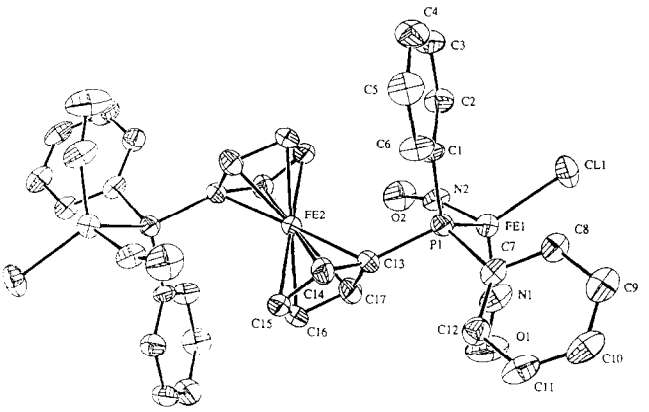

Fig. 1. Molecular structure of $[\{Fe(NO)_2Cl\}_2(\mu\text{-}FcP_2)]$ (**2**).

The parallel cyclopentadienyl rings adopt a staggered configuration with the two phosphorus atoms oriented *trans* with respect to the ferrocene moiety.

The coordination geometry at the nitrosyl iron atoms, Fe(1), is a distorted tetrahedron. The P–Fe–Cl angle of 105.76(7)° falls between the P–Fe–Cl angles of 101.75(9)° for the analogous dppe complex, $[\{Fe(NO)_2Cl\}_2(\mu\text{-dppe})]$ [11] and 112.0(1)° in the monomeric $[Fe(NO)_2Cl(PPh_3)]$ [12]. This variation in the P–Fe–Cl bond angles is consistent with the steric demands of the phosphine groups, which fall in the series $PPh_3 > Ph_2P(C_5H_4) > Ph_2PCH_2$. The bond distances and angles for each $Fe(NO)_2$ moiety are within the expected range [11,12]; the Fe–N–O angles are 163.3(5) and 163.6(4)° and the N–O bond lengths 1.183(7) and 1.178(6) Å. Finally, the two nitrosyl ligands in **2** adopt an "attracto" conformation [13], the O–Fe–O angle of 102.3° being less than the N–Fe–N angle of 114.6°.

The geometry of the Fe(1)–P–C(13)–C(13')–P'–Fe(1') bridge is totally reminiscent of the Fe–P–C–C–P–Fe bridge in $[\{Fe(NO)_2Cl\}_2(\mu\text{-dppe})]$ [11]. The Fe–P and P–C(bridge) distances in **2** are 2.3469(18) and 1.831(7) Å respectively, compared with 2.356(2) and 1.833(7) Å in the dppe analogue. As illustrated in Scheme 2, the only significant difference arises from the increase steric demand of the ferrocene group in **2** compared with two methylene groups in the dppe complex which results in an (NO)Fe...Fe(NO) distance of 8.36 Å in **2** in spite of 6.81 Å in the dppe complex.

Complex **2** and its dppe analogue differ slightly in the geometry of the Fe–NO moieties and this could have been significant for the reactivity of the nitrosyls. Thus the nitrosyls are more bent, i.e. less NO^+ in character, in **2** than in the dppe-bridged dimer; the Fe–N–O angles are 163.3(5) and 163.6(4)° in **2** compared with 165.7(6) and 169.5(7)° in $[\{Fe(NO)_2Cl\}_2(\mu\text{-dppe})]$. In contrast, the N–O bond lengths in **2** (1.183(7) and 1.178(6) Å) are not significantly different from those in the dppe complex (1.161(9) and 1.156(8) Å). The structural data for **2** thus indicate that the pres-

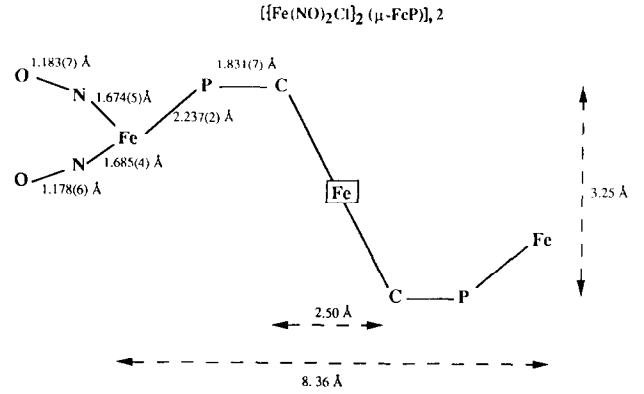

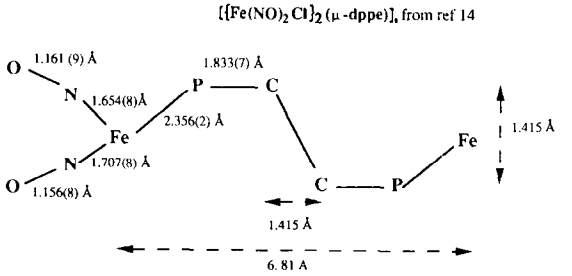

Scheme 2.

ence of the FcP_2 ligand does not result in significant NO activation.

3.2. Reactivity of $[\{Fe(NO)_2Cl\}_2]$ in the presence of FcP_2

3.2.1. Towards dioxygen: Fe–NO → Fe–NO_3 oxidation

Bubbling dioxygen into dichloromethane or acetonitrile solutions of $[\{Fe(NO)_2Cl\}_2]$ dimer **1** in the presence of FcP_2 (two equivalents) caused a rapid change from black to brownish. Treatment of the reaction mixture afforded stoichiometric amounts of **5** which analyses as $Fe(NO_3)_2(Cl)(O_2P_2Fc)$. The IR spectra of **5** (KBr pellets) showed the complete disappearance of the nitrosyl bands, while new absorptions were observed at 1521, 1288 and 828 cm^{-1}, in the regions generally assigned to bound nitrates [14]. The oxidation of bis(diphenylphosphino)ferrocene to bis(oxodiphenylphosphorano)ferrocene is indicated by a strong absorption band at 1148 cm^{-1} assignable to a coordinated phosphoryl group. The formulation of **5** was further confirmed through its independent preparation from anhydrous iron(III) chloride, FcP_2O_2 and silver nitrate, and the subsequent comparison of the corresponding IR spectra.

3.2.2. Towards an excess of FcP_2

When two equivalents of FcP_2 were allowed to react with $[\{Fe(NO)_2Cl\}_2]$ (**1**) in toluene at RT, or when **2** was allowed to react with one equivalent of FcP_2, two species could be isolated: a green complex **3**, insoluble in toluene but soluble in CH_2Cl_2 and CH_3CN, and a red compound **4**, readily soluble in toluene, CH_2Cl_2 and CH_3CN.

Addition of an equal volume of pentane to a toluene solution of **4** produced red crystals of $[Fe(NO)_2(FcP_2)]$ characterized by NO stretches at 1707 and 1659 cm^{-1}, by a single ^{31}P NMR resonance at $\delta = 58$ ppm, by elemental analyses and an X-ray structural analysis.

Adduct **3** is extremely sensitive to traces of air, and we have so far been unable to obtain satisfactory elemental analyses for it. The presence in the IR spectrum of **3** of a strong vibration at 1144 cm^{-1} assignable to a coordinated phosphoryl group (υ(P=O) = 1190 cm^{-1} in free FcP_2O_2) shows that the diphosphine ligand has been oxidized. A single NO stretch is observed at 1788 cm^{-1}. The presence of two distinct P–C stretching bands at 1094 and 1119 cm^{-1}, corresponding to phosphine and to phosphine oxide respectively, suggests that FcP_2 has been converted to FcPPO.

The ESR spectrum of a CH_2Cl_2 solution of **3** at RT consists of a single broad line (120 G peak to peak) at $g = 2.02$. No ^{31}P hyperfine coupling was resolved. However, the presence of the mono-oxygenated FcPPO ligand in **3** is further supported by the ^{31}P NMR spectra measured in CH_2Cl_2, which contain two signals in a 1:1 area ratio at 34 and 40 ppm which we have tentatively assigned to coordinated P and PO respectively. Mainly on the basis of the IR data, **3** is formulated as $[Fe(NO)Cl_2(FcPPO)]$. We had previously found a similar behaviour for $[Fe(NO)_2Cl]$ in the presence of two equivalents of dppe ligand [15].

It is note worthy that **3**, in the presence of even the slightest traces of air, forms $[FeCl_4][FeCl_2(FcP_2O_2)_2]$ (**6**) where the two phosphino groups have been oxidized to two phosphoryl units. Compound **6** was identified through comparison with an authentic sample prepared from anhydrous $FeCl_3$ and FcP_2O_2.

3.2.3. Direct formation of 3 from 4

The relative amounts of **3** and **4**, obtained from the reactions of either **2** with one equivalent of FcP_2 or **1** with two equivalents of FcP_2, were found to vary as a function of the reaction time. Thus, when **2** and FcP_2 were left into contact for 1 h, **3** and **4** accounted for 27 and 67%, respectively of the starting iron nitrosyl (**3**:**4** ratio, 0.4) while, after 12 h contact, the **3**:**4** ratio increased to 1.7.

Hence, it is reasonable that **3** was formed from **4** in the reaction medium. Fully consistent with this hypothesis, when **4** was allowed to react with chlorine generated in situ, it afforded **3** selectively:

$$[Fe(NO)_2(FcP_2)] + Cl_2 \rightarrow [Fe(NO)Cl_2(FcPPO)] \quad (1)$$

3.2.4. Molecular structure of $[Fe(NO)_2(FcP_2)]$ (4)

The molecular structure of **4** is illustrated in Fig. 2 with selected bond angles and bond distances gathered in Table 5. The geometry of the iron nitrosyl moiety in **4** is that of a distorted tetrahedron. Iron atom Fe(2) is coordinated to two nearly linear nitrosyl ligands (176.8(5) and 177.8(5)°) and to the two phosphorus donors of FcP_2. The Fe–N and N–O bond lengths and N–Fe–N and Fe–N–O angles are close to those found in other iron dinitrosyl complexes containing linearly coordinated NO groups [16]. The $Fe(NO)_2$ group is planar; the N–Fe–N angle of 125.1(3)° is larger than the O–Fe–O angle of 122.9(1)°, indicating that the $Fe(NO)_2$ moiety adopts again an attracto conformation.

Extensive studies on complexes containing variously substituted ferrocenyl phosphine ligands have shown a peculiarly large bite for this type of diphosphine, resulting in quite large P–M–P angles [17]. Correspondingly, the average M–P distances are large in comparison with the values observed in similar complexes with chelating diphosphines [17]. Therefore the large 101.66(6)° P–Fe(2)–P angle in **4**, to be compared with the 85.92° value in the analogous dppe derivative [11], is not surprising. The Fe(2)–P bond lengths of 2.2560(18) and 2.2635(18) Å in **4** compare favourably with the M–P distances found in FcP_2 iron carbonyl complexes [17c,18].

3.3. Oxygen transfer from the iron nitrato complex 5

In order to test the oxidizing step in the (Fe–NO)–($Fe–NO_3$) cycle, the oxygen transfer ability of the nitrato moieties in $[Fe(NO_3)_2(Cl)(O_2P_2Fc)]$ (5) towards an organic substrate was evaluated under a strictly controlled argon atmosphere. Complex **5** was found to be most reluctant to react stoichiometrically with olefins under anaerobic conditions. No reaction was observed between **5** and cyclohexene (olefin:Fe, 10:1) after 72 h RT under argon. The unaltered nitrato complex was recovered quantitatively.

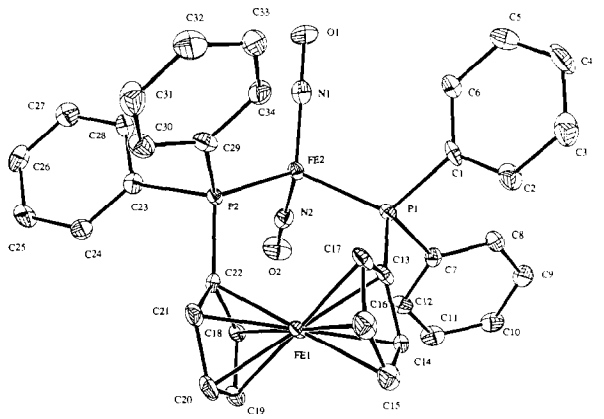

Fig. 2. Molecular structure of $[Fe(NO)_2(FcP_2)]$ (**4**).

On the contrary, **5** reacts rapidly with phosphines in the absence of dioxygen. IR monitoring of the reaction of **5** with a tenfold excess of PPh_3 under argon at RT showed the rapid disappearance of the NO_3 vibrations together with the appearance of bands due to $OPPh_3$ ($\upsilon(P{=}O) = 1188\ cm^{-1}$). Besides the formation of $OPPh_3$, the reaction gives a mixture of iron species which could not be separated for further characterization. It should be noted that no $\upsilon(NO)$ bands could be detected in the IR spectrum of the product mixture, while specific analysis by the Griess reagent [19] indicated the presence of traces of NO_2^- and no NO_3^-.

3.4. Complex 5 as a catalyst in cyclohexene oxidation

Complex **5** catalyses the aerobic oxidation of cyclohexene mainly to 2-cyclohexene-1-one and 2-cyclohexene-1-ol, with cyclohexene oxide being formed only in traces. These organic products were identified by GC–MS and their spectra compared with those of authentic samples.

The formation of cyclohexenone and cyclohexenol, which are typical autoxidation products of cyclohexene, suggests that **5** is simply decomposing cyclohexenyl hydroperoxide, a classical behaviour for metal complexes [20–23]. Compound **5** favours cyclohexenone over cyclohexenol and this selectivity is increased on going from dichloromethane (cyclohexenone: cyclohexenol, 60:40) to acetonitrile (cyclohexenone: cyclohexenol, 70:30) as a solvent.

4. Discussion

The addition of FcP_2 to $[\{Fe(NO)_2Cl\}_2]$ first yields the binuclear complex $[\{Fe(NO)_2Cl\}_2(\mu\text{-}FcP_2)]$ (**2**). This result is consistent with the ability of the $Fe(NO)_2Cl$ moiety to chelate bidentate phosphines such as dppe or 1,2-bis(diphenylphosphino)ethene [15]. The molecular structure of **2** shows no really significant difference between **2** and its dppe analogue, apart from the increased steric demand of the bridging Fc group compared with $(CH_2)_2$ in the dppe complex; in both complexes the nitrosyls are essentially NO^+ in character.

The reaction of **2** with dioxygen yielded the nitrato complex **5** and no nitro species. A key step in the reaction of dioxygen with metal nitrosyl complexes to produce a nitro compound is thought to be the generation of an NO^- complex [24]. Thus the reaction of $[Co(NO^+)L_4]$ with dioxygen in the presence of a base which generates a reactive NO^- species leads to the exclusive formation of a nitro derivative [25]. We believe that the nitrosonium character of the NO group in **2** precludes this mechanism and that dissociation of

NO and its subsequent capture by molecular oxygen are predominantly responsible for the formation of nitrates [26].

This behaviour is closely related to what we observed previously in the presence of monodentate L (PPh_3 [1], hexamethylphosphoric triamide (HMPA) [2]), or bidentate LL ligands (bipyridine [3,4] and dppe [5]) where we had found the nitrosyl ligands in $[\{Fe(NO)_2X\}_2]$(X = Cl or I) are oxidized by molecular oxygen to nitrates in the easily isolated complexes $[Fe(NO_3)X_2L'_2]$ or $[Fe(NO_3)_2XL'_2]$ (L' = $OPPh_3$, O_2dppe, HMPA or bipy). In these nitrato complexes, any phosphine present has also been oxidized to coordinated phosphine oxides.

That **2** behaves like its dppe analogue, i.e. that the presence of ferrocene has no influence on the $Fe(NO)_2Cl$ moiety in **2** compared with its phosphine analogues, is further confirmed by its reactivity toward an excess of phosphine. Compound **2** was found to react with an excess of FcP_2 first to yield $[Fe(NO)_2(FcP_2)]$, (**4**). Indeed $[Fe(NO)_2Cl(L)]$ mononuclear nitrosyl complexes have been found to react with an excess of L, to give the diamagnetic $[Fe(NO)_2(L)_2]$, and the proposed mechanism postulates formation of intermediate $[Fe(NO)_2XL_2]$, a 19-electron compound, which can react in two pathways, namely to the products or back to the reagents [27]. Such behaviour has been observed with phosphine of various basicities, such as L = PPh_3, P^nBu_3, and $P(O^iPr)_3$:

$$[Fe(NO)_2XL] + L \rightleftarrows [Fe(NO)_2XL_2] \rightleftarrows [Fe(NO)_2L_2] + X$$

In the case of the bidentate phosphine FcP_2, our results show that the corresponding $[Fe(NO)_2L_2]$ complex **4** reacts further with X to yield **3**. This behaviour parallels that of the dppe analogue.

The nitrato ligands in $[Fe(NO_3)_2Cl(O_2P_2Fc)]$ (**5**) are capable of transferring oxygen to phosphines. This oxygen transfer does not regenerate the nitrosyl moiety, which is markedly different from what we have observed in the presence of monodentate phosphorus ligands, where oxygen transfer from $[Fe(NO_3)_2Cl(HMPA)_2]$, $[Fe(NO_3)_2Cl(OPPh_3)_2]$ or $[Fe(NO_3)Cl_2(HMPA)_2]$ yields nitrosyls [1,2]. Although further work is required to understand and improve the reactivity found for these nitrato complexes, our results seem to indicate that the nitrato groups in **5** might be transformed into nitro or nitrito groups through oxygen transfer to PPh_3. Traces of NO_2^- were in the reduced iron residue left after the oxygen transfer. That only small amounts of $Fe-NO_2$ were found after oxygen transfer from the $Fe-NO_3$ moiety in **5**, is probably due to the known instability of iron nitrites. They have been isolated only in the case of iron picket-fence porphyrin complexes where the ligand-binding site is protected [28].

In the presence of **5**, cyclohexene is preferentially oxidized into the α,β-unsaturated ketone, showing that allylic oxidation is the main process. The selectivity found for cyclohexene is characteristic of autoxidation, a reaction that has long been known to be catalysed by transition metal complexes [20–23].

Acknowledgments

We are grateful to the Centre National de la Recherche Scientifique for financial support of this work.

References

[1] F. Tomi, H. Li Kam Wah and M. Postel, *New J. Chem., 12* (1988) 289.
[2] H. Li Kam Wah, M. Postel and F. Tomi, *Inorg. Chem., 28* (1989) 233.
[3] H. Li Kam Wah, M. Postel, F. Tomi, L. Mordenti, D. Ballivet-Tkatchenko, F. Dahan and F. Urso, *New J. Chem., 15* (1991) 629.
[4] H. Li Kam Wah, M. Postel, F. Tomi, F. Agbossou, D. Ballivet-Tkatchenko and F. Urso, *Inorg. Chim. Acta, 205* (1993) 113.
[5] V. Munyejabo, P. Guillaume and M. Postel, *Inorg. Chim. Acta, 221* (1994) 133.
[6] D. Ballivet-Tkatchenko, C. Billard and A. Revillon, *J. Polym. Sci., 19* (1981) 1697.
[7] V. Munyejabo, M. Postel, J.L. Roustan and C. Bensimon, *Acta Crystallogr. Sect. C, 50,* (1994 part II, 224).
[8] D.F. Grant and E.J. Gabe, *J. Appl. Crystallogr., 11* (1978) 114.
[9] E.J. Gabe, F.L. Lee and Y. Lepage, *J. Appl. Crystallogr., 22* (1989) 384.
[10] D. Ballivet-Tkatchenko, B. Nickel, A. Rassat and J. Vincent-Vaucquelin, *Inorg. Chem., 25* (1986) 3497.
[11] H. Li Kam Wah, M. Postel and M. Pierrot, *Inorg. Chim. Acta, 165* (1989) 215.
[12] J. Kopj and J. Schmidt, *Z. Naturforsch., 30b* (1975) 149.
[13] R.L. Martin and D. Taylor, *Inorg. Chem., 15* (1976) 2970.
[14] N. Nakamoto, *Infrared and Raman Spectra of Inorganic and Coordination Compounds,* Wiley–Interscience, New York, 3rd eds., 1978, pp. 244–247.
[15] P. Guillaume, H. Li Kam Wah and M. Postel, *Inorg. Chem., 30* (1991) 1828.
[16] J.K. Enemark and R.D. Feltham, *Coord. Chem. Rev., 13* (1974) 339.
[17] (a) I.A. Butler, W.R. Cullen, T.J. Kim, S.J. Rettig and J. Trotter, *Organometallics, 4* (1985) 972; (b) T.M. Miller, K.J. Ahmed and M.S. Wrighton, *Inorg. Chem., 28* (1989) 2347; (c) L. K. Liu, S.K. Yen and C.C. Lin, *Bull. Inst. Chem., Acad. Sin., 35* (1988) 45; (d) M.I. Bruce, I.R. Butler, W.R. Cullen, G.A. Koutsantonis, M.R. Snow and E.R.T. Tiekink, *Aust. J. Chem., 41* (1988) 963; (e) M. Adachi, M. Kita, K. Kashiwabara, J. Fujita, N. Litaka, S. Kurachi, S. Ohba and D.M. Jin, *Bull. Chem. Soc. Jpn., 65* (1992) 2037; (f) U. Casellato, B. Corain, R. Graziani, B. Longato and G. Pilloni, *Inorg. Chem., 29* (1990) 1193; (g) U. Casellato, D. Ajo, G. Valle, B. Corain, B. Longato and R.J. Graziani, *Crystallogr. Spectrosc. Res., 18* (1988) 583; (h) B. Longato, G. Pilloni, G. Valle and B. Corain, *Inorg. Chem., 27* (1988) 956; (i) P.F. Kelly, A.M.Z. Slawin, D.J. Williams and J.D. Woollins, *Polyhedron, 7* (1988) 1925; (j) A.L. Bandini, G. Banditelli, M.A. Cinellu, G. Sanna, G. Minghetti, F. Demartin and

M. Manassero, *Inorg. Chem., 28* (1989) 404; (k) G. Bandoli, G. Trovo, A. Dolmella and B. Longato, *Inorg. Chem., 31* (1992) 45.
[18] T.J. Kim, S.C. Kwon, Y.H. Kim, N.H. Heo, M.M. Teeter and A. Yamano, *J. Organomet. Chem., 426* (1991) 71.
[19] G. Charlot, *Chimie Analytique Quantitative,* Masson, Paris, 1974.
[20] R.A. Sheldon and J.K. Kochi, *Metal-catalyzed Oxidations of Organic Compounds,* Academic Press, New York, 1981.
[21] I. Tabushi and N. Koga, *J. Am. Chem. Soc., 101* (1979) 6456.
[22] H. Ledon, *C.R. Acad. Sci., Paris*, (1979) 288.
[23] J. Muzart, *Bull. Soc. Chim. Fr., 1* (1986) 65.
[24] S.M. Bhaduri, I. Bratt, B.F.G. Johnson, A. Khair, J.A. Segal, R. Walters and C. Zuccaro, *J. Chem. Soc., Dalton Trans.*, (1981), 234.
[25] S.G. Clarkson and F. Basolo, *Inorg. Chem., 12* (1973) 1528.
[26] M.P. Doyle, R. Pickering and B.R. Cook, *J. Am. Chem. Soc., 104* (1982) 3392.
[27] S. Pignataro, G. Distefano and A. Foffani, *J. Am. Chem. Soc., 92* (1970) 6425.
[28] M.G. Finnegan, A.G. Lappin and W.R. Scheidt, *Inorg. Chem., 29* (1990) 181.